Effect of Clay Modifier on the Structure and Transport Properties in Polyurethane/Clay Nanocomposites as Barrier Materials

Ramesh, S.*+; Kamalarajan, P.

Department of Chemistry, R.M.D. Engineering College, Kavaraipettai 601206, Tamilnadu, INDIA

Punithamoorthy, K.

Department of Chemistry, Government Arts College, Nandanam, Chennai 600035, Tamilnadu, INDIA

ABSTRACT: *In this study, nanocomposites of Thermoplastic Polyurethane (TPU) clay are synthesized and used as a gas barrier property. The NCO-terminated TPU prepolymer was prepared by solution polymerization method using a 1:2 ratio of Polyethylene glycol (PEG_{2000}) and Tolylene 2,4-diisocyanate (TPI). Organo-modified montmorillonite clay, Cloisite 25A(C25A) was used as ample compatibilization with PEG/TPI matrix. The prepared nanocomposite was characterized by Fourier Transform InfraRed (FT-IR) spectroscopy, X-Ray Diffraction (XRD), Scanning Electron Microscope (SEM), and ThermoGravimetric Analysis (TGA). The main functional group peaks of the nanocomposite materials are observed in FT-IR spectroscopy. The nanocomposites exhibited better thermal stabilities than pristine Polyurethane which is investigated by TGA. Thermal stability in the sample with 5 wt.% of TPU/C25A-5 material has improved up to 70ºC. The XRD results have confirmed the penetration of clay into TPU matrix, with the disappearance of the characteristic peak ($2\theta = 4.81^{o}$) corresponding to the d-spacing of the organoclay. SEM analysis confirmed the dispersion of nanoclay in TPU matrix. The mechanical properties of nanocomposites such as the tensile strength and Young's modulus of TPU/Cl25A nanocomposites were increased with increasing clay percentage. The gas permeability test was studied using a Membrane separation testing unit. Significant improvements in barrier properties were observed. A remarkable decrease was seen in polyurethane incorporated with 5 Wt.% organoclay when tested with oxygen and nitrogen gas.*

KEYWORDS: *Polyurethane; Organoclay; Nanocomposites; Gas barrier properties.*

INTRODUCTION

One of the most potential materials in recent decades is Polymer-Layered silicate Nanocomposite (PLN). PLN is a new class of materials produced by the dispersion of a percentage weight of clay in a polymer matrix that differs from the nanoscale [1,2]. Because of the high interaction between components, they were synthesized using a simple, low-cost approach and superior to traditional materials. [3]. Fire retardancy, optical, mechanical, and

***** *To whom correspondence should be addressed.*
+ *E-mail: rameshche@gmail.com*
1021-9986/2022/10/3542-3552 11/$/6.01

barrier properties of polymer/clay nanocomposite are employed in various consumer products like cable, automobile, electronics, packaging, coatings, bottle batteries, and the film sector [4-6]. Delaminating of nanoclays using melt shearing, in situ polymerization, and the sol–gel method have all been used to synthesize Polymer clay nanocomposite. Nanoclay dispersion improves bulk polymer properties such as thermal stability, gas barrier, mechanical strength, and flame retardancy. [7-10]. The main causes of clay minerals as reinforcing materials are their low cost, density, high availability, aspect ratio, and large surface area, which enhance the properties of the polymer. Montmorillonite (Mt) is a member of the 2:1 phyllosilicate. Cloisite 25A (C25A) and organoclay obtained by Mt are modified by reinforcing polymeric matrices of methyl tallow bis-2-hydroxy ethyl quaternary ammonium. C25A is better compatible with polyurethane (Pu) in comparison to other organo-modified clay Cloisite 10A, Cloisite 20A [11-13].

Polyurethane (Pu) is a potential elastomer with outstanding qualities that provide excellent performance and processing flexibility. TPU is made up of two parts: soft and hard. The soft component is commonly made up of bio-based polyether or polyester, while the hard part comprises diisocyanate and chain extenders [14,15]. The property of Pu can be tailored by the types of raw materials, their composition, and processing conditions. Pu is widely used for coatings, adhesives, sealants, foams, and fibers due to its versatile properties. PU clay materials have attracted attention for inferior gas barrier properties. The micro-phase separation of Pu which is the difference in polarity and thermodynamic incompatibility of the two segments is the main reason for inferior gas barrier properties [16-18]. The gas barrier properties of the polymer nanocomposite improve mainly because of three reasons, (i) an increase in tortuous path, (ii) an increase in interaction between polymer and clay by bonding, (iii) an increase in movement of polymer chains in the presence of intercalated or exfoliated clay [19]. A series of PE nanocomposites containing Cloisite 20A and graphite nanoparticles were prepared and introduced as potential materials for the production of polymeric pipes in natural gas transfer systems [20].

Many studies and scientists have concentrated on improving the gas barrier properties of PU by altering the basic materials and formulations [21,22]. The effect of hard segment content on the thermal, morphological, and mechanical properties of polyurethane polymers has been discussed based on diol and chain extenders [23]. Moreover, many researchers have utilized nano-clay or functionalized graphene nanocomposite to improve the gas barrier properties of PU. When compared to pure PU, *Peretz Damari et al.* found that nanocomposite based on graphene generated by the solution approach performed better [24,25]. Poly(vinyl alcohol)/nanoclay nanocomposite foams containing different concentrations of cloisite 30B were used for water absorption capacity [26]. The Processing technique plays a significant role in improving the properties of final polymer clay nanocomposites. Many kinds of literature report that solution mixing gives the best results than melt mixing. The dispersion of clay minerals in the polymer matrix is still a big challenge in melt mixing [27]. *Finnigan et al*. reported that adding 3% and 7% weight of Cloisite 30B to TPU, resulted in a decrease in tensile strength and elongation due to the degradation of Pu in the melt compounding process [28]. As a result, solution mixing was performed in this investigation to achieve homogeneous clay dispersion in the Pu matrix. *B. Adak et al*. are reported the effect of two different organoclay and their He gas barrier properties of Pu nanocomposites [29]. The water absorption properties of 3% of nanoclay with CMC/PVA nanocomposites are reported [30].

In this study, we synthesized Polyurethane /clay nanocomposites are used as a gas barrier property. The effect of nano-clay was evaluated on morphology and the mechanical properties of PU/C25A nanocomposites. To the best of our knowledge, the role of organo-modified clay on the behavior of PU/Cl25A nanocomposite material has not been reported yet.

EXPERIMENTAL SECTION

Materials

All reagents are used as an analytical grade. Polyethylene glycol (PEG_{2000}) and the Potassium salt of hydroquinone sulphonic acid are procured from Fluka, India. Isophorone-diisocyanate (IPDI) and Tolylene 2,4-diisocyanate, (TDI) are purchased from Sigma Aldrich, India. Dibutyltin-dilaurate (DBTDL) is obtained from Fluka. N, N-dimethyl formamide (HPLC grade) was purchased from Sisco Research Laboratories, Mumbai, India. Cloisite 25A (Sodium montmorillonite modified with dimethyl hydrogenated tallow,2-ethylhexyl

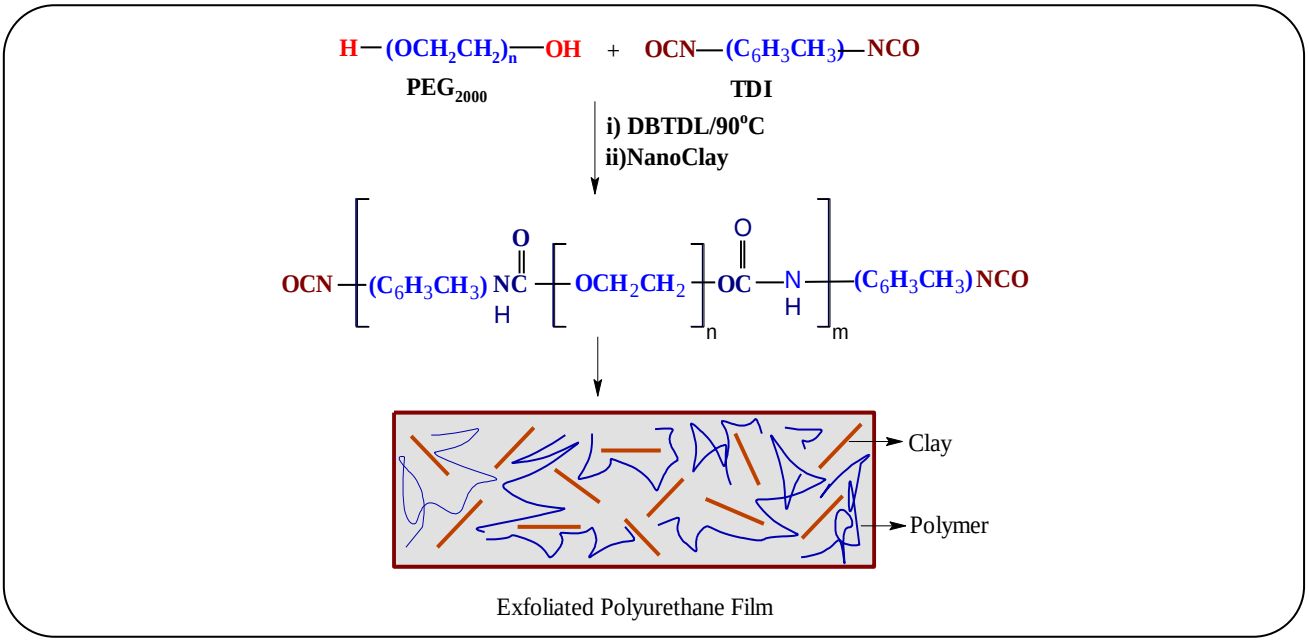

Fig. 1: The reaction procedure and the structure of TPU/C25A nanocomposites synthesized in the study.

quarternary ammonium cation) was received from Southern Clay, USA. Initially, clay was dried in a hot air oven at 80 ºC for 6 hours to remove moisture content. Dimethylformamide (DMF) (Merck, India) was used as such without further purification.

Synthesis of TPU clay nanocomposite

The TPU clay nanocomposite is prepared as described earlier in the literature [31]. Polyethylene glycol (0.01 mol/L) was taken in a three-necked reaction kettle and dissolved in 50 mL of Dimethylformamide. After swelling of Polyethylene glycol in DMF calculated quantity of Cloisite 25A (1 Wt.% regarding the monomer) and Tolylene 2,4- diisocyanate (TDI) (0.02 mol/L) was slowly added to a reaction vessel. The potassium salt of hydroquinone sulphonic acid (0.0065g) was dissolved in DMF and added dropwise at 50ºC for chain extension. The heating was continued until the theoretical isocyanate content of 4-5% was reached, as determined by the dibutyl-amine method and from the disappearance of IR absorption of the NCO group at 2270 cm^{-1}. The reaction mixture is heated up to 80 ºC under a nitrogen atmosphere for 4 hours. TPU/C25A nanocomposite film is obtained by pouring the emulsion onto a Teflon mold. The experiment is repeated with 3, 5, and 7 Wt.% of clay, and the prepared composite material is dried and various analytical techniques characterize it. The reaction procedure and the structure of TPU/C25A nanocomposites synthesized in this study are given in Fig. 1. The codes and composition of the nanocomposite are given in Table 1.

Characterization

The FT-IR spectra of clay nanocomposite are analyzed using a Nicolet impact 400 FT-IR spectrometer. The X-Ray Diffraction (XRD) measurements of the clay and nanocomposites are taken with the Rigaku Miniflex diffractometer (30 kV,10 mA) with Cu Kα radiation (λ = 1.54 Å) at a scanning rate of 2 ºC/min at room temperature. The spectra are recorded in the 2θ range 0 to 15 degrees. The basal spacing of the nanocomposites is calculated using Bragg's equation. The composite specimens are analyzed by X-ray diffraction using films of 2 mm thickness that are obtained at 180 ºC compression molding. The thermal stability of the polymer clay nanocomposites is performed on the Perkin Elmer, Thermal Gravimetric Analysis (TGA) system at a 20 ºC/min heating rate in N_2 atmosphere. The sample was heated at room temperature to 800 ºC. Scanning electron microscopic images of fractured surfaces of tensile specimens are carried out using the JEOL JEM-5800 with an acceleration voltage of 20 kV. Mechanical studies are measured using a UTM Universal Testing Machine (Instron-3369, UK). A load of 100N is applied at a crosshead speed of 50 mm/min. The dumb-bell shaped specimens with a diameter of 15 mm wide

Table 1: Composition and codes of Polyurethane /Clay Nanocomposites.

Sample Code	Composition				
	NCO / OH ratio	TDI	PEG	Clay Wt.%	Hard Segment (mol %)
TPU	1.0	75	25	0	21
TPU/C25A-1	1.1	75	25	1	22
TPU/C25A-3	1.3	75	25	3	23
TPU/C25A-5	1.5	75	25	5	24
TPU/C25A-7	1.7	75	25	7	25

at the two ends and 10 mm wide at the neck with a thickness ranging from 1.1 to 2.9 mm are used to carry out the test as per ASTM D: 638 test procedures. The permeation study is done at the constant pressure method using a membrane separation unit.

RESULTS AND DISCUSSION

FT-IR Analysis

The Structural characteristics of pure TPU and TPU/C25A nanocomposites are carried out using FT-IR analysis [32]. The infrared spectrum of the TPU and TPU1 nanocomposite are given in Fig. 2. FT-IR spectra of the described samples were carried out in the region 4000-500 cm^{-1} at room temperature. The presence of a characteristic peak at 3300 cm^{-1} is assigned to the NH bending vibration of urethane which is produced by the reaction of the NCO and OH group. The following absorption bands of 660 cm^{-1} (CH out of plane bending), 1156 cm^{-1} (C-O stretching), 1390 cm^{-1} (CH bending), 1458 cm^{-1} (CH_2 plane scissoring), 2953 cm^{-1} (CH_2 symmetric stretching) respectively are shown by TPU spectrum. The bands occur around 1050 - 1300 cm^{-1} which corresponds to the C-O stretching vibration of the ester group.

The characteristic absorption bands of TPU/C25A-1 weight percentage for the nanocomposites are revealed. The following are characteristic bands 660 cm^{-1} (C-H vibration of aromatic ring), 2975 to 2888 cm^{-1} (CH stretching), 1088 cm^{-1} (Si-O asymmetric stretching), 1259,1088,1018 cm^{-1} (C-O stretching vibration of ester group) respectively. The CH stretching of nanocomposite does not change, and it indicates the clay particle did not react with H bond formation by urethane –NH groups. FT-IR spectra demonstrated the effective complexation and strong interaction between clay and polymer.

Wide angle X-ray diffraction Analysis

The XRD measurement is used to calculate the basal spacing (d_{001}) at peak positions according to Bragg's law . The wide-angle XRD patterns of pure clay and TPU/C25A nanocomposite of different wt.% is shown in Fig. 3. Polymer/clay nanocomposites are formed by the insertion of polymer chains between the clay layers with increased gallery space [33]. A shift in the d_{001} peak of clay in the XRD spectrum is associated with the formation of intercalated structure, while the disappearance of this peak is indicative of an exfoliated structure in nanocomposites. The organomodified MMT clay ie Cloisite 25A shows a 001 characteristic peak at $2\theta = 4.81^{o}$, corresponding to the silicate-interlayer spacing value of 18.5 Å. However, these TPU/C25A nanocomposites show the absent of a strong peak up to 6º angle in the spectral range which indicates that the insertion of polyurethane exfoliated the silicate layer of the Cloisite 25A as a bulk state. The results show that the clay contents are homogeneously exfoliated and randomly dispersed in the TPU matrix.

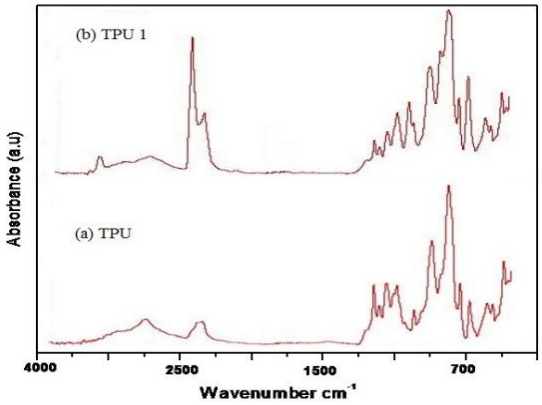

Fig. 2: FT- IR spectra of neat TPU and TPU/C25A (TPU1) nanocomposite.

Thermogravimetric analysis

The TGA thermograms of TPU and TPU/C25A with different Wt.% of clay nanocomposites at 20 °C under

Table 1: Thermal decomposition of pure TPU and TPU/C25A nanocomposites.

TPU/C25A Nanocomposites with various C25A clay content wt.%					
	TPU	TPU/C25A-1	TPU/C25A-3	TPU/C25A-5	TPU/C25A-7
T_1 °C	207.42	308.24	331.46	356.76	341.68
T_2 °C	402.34	492.43	505.07	532.36	512.42
Residue wt.%	19.24	21.47	24.87	27.27	23.62

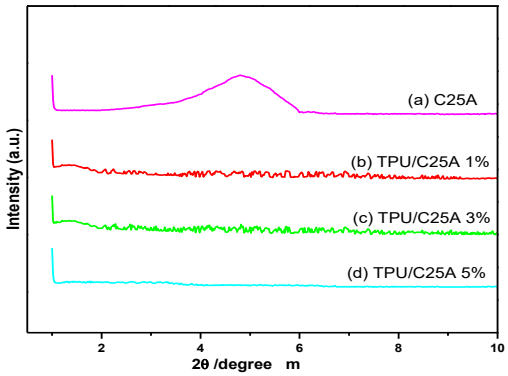

Fig. 3: XRD spectra of: (a) Cloisite 25A clay and prepared nanocomposites at different concentrations of clay nanocomposites b) TPU/C25A 1% (c)TPU/C25A 3% (d) TPU/C25A 5%.

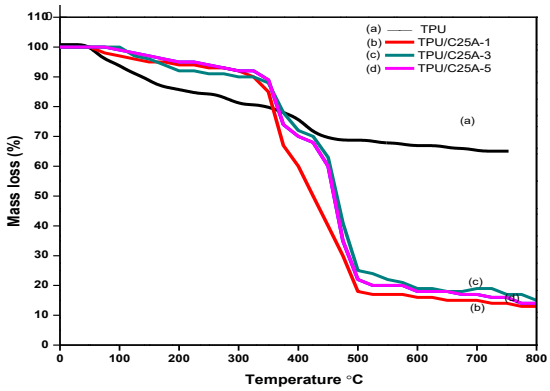

Fig. 4: TGA thermograms of neat (a) pure TPU (b) TPU/C25A -1 (c) TPU/C25A -3 (d) TPU/C25A -5 nanocomposites.

nitrogen is illustrated in Fig. 4. The values of TPU and TPU/C25A are given in Table 2. Generally, the thermal stability of the nanocomposites is affected by organoclay in two ways, one is due to degradation of polymer by catalysis effect and another one is oxygen increasing the stability by barrier property [34]. The present study shows that the barrier effect is predominant as a low fraction of clay was added to the polymer matrix.

Pure TPU/C25A undergoes two different stages of thermal degradation. The first stage is attributed to the acetate group elimination, which occurs degradation temperature range up to 300 to 400 °C. The second stage is the degradation of the main chain. The nanocomposites showed no weight loss under 207 °C and all the samples undergo decomposition commenced at around 300 °C. This result reveals that the TPU is completely anhydrous and possess relatively good thermal stability. Moreover, it was found that the TPU/C25A nanocomposites exhibited a slightly higher thermal decomposition temperature, i.e., 308 °C, compared to TPU adduct 207 °C respectively. The TPU/C25A nanocomposite samples left a residue of about 22 % at 800 ° C whereas the TPU adduct left about 19 % at the same temperature. Such results indicate that 85% of the initial clay added was quantitatively introduced into the TPU adduct as an exfoliated structure and it might be changing the degradation mechanism of TPU/C25A nanocomposites under high temperatures.

T_1 and T_2 is the decomposition temperature at 20% and 60% of the weight loss, respectively. Pure TPU has a temperature of T_1 = 207 ° C and T_2 = 402 ° C, whereas TPU/C25A nanocomposites have increased the temperature from 320 ° C and 500 ° C, respectively. As a result, at the maximum decomposition temperature, the highest percentage of clay is successfully achieved. Finally, the TGA results suggest that the mobility of the polymer segments and clay at interfaces are partially suppressed by the interaction between them, resulting in a delay in polymer degradation. The thermal stability of the nanocomposites has improved when compared to that of pure TPU confirming positive structural changes [35,36].

Scanning electron microscopy analysis

Scanning Electron Microscopy is used to analyze the modified clay dispersion in TPU nanocomposites as the initial stage. Scanning electron images of TPU with

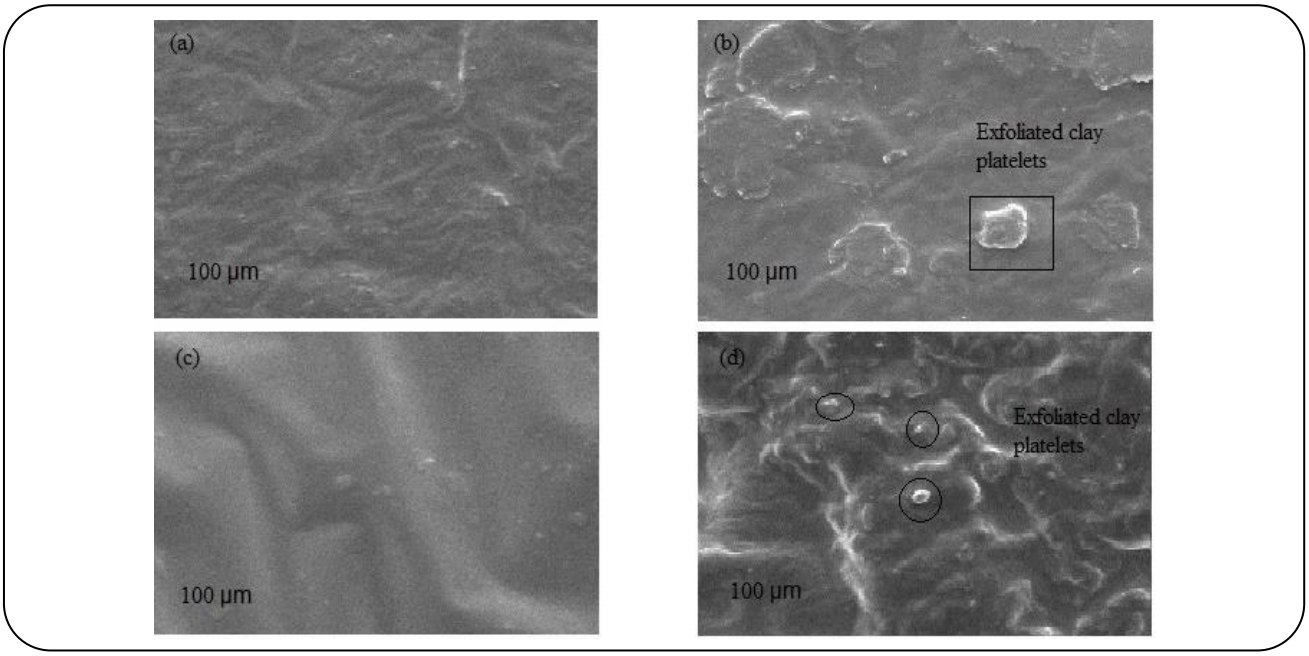

Fig. 5: Scanning electron micrographs of (a) TPU (b) TPU/C25A -1 (c) TPU/C25A - 3 (d) TPU/C25A - 5 nanocomposites.

various clay weight contents are shown in Fig. 5. The SEM images are used to examine the film surfaces of nanocomposites and calculate the size of clay filler agglomerates on the film surfaces. Under this magnification, the clay particles are equally dispersed inside the TPU matrix structure in the presence of tiny agglomerates, whereas the SEM images of pure TPU and TPU/C25A nanocomposites show significant variances. These clay particles range in size from 0.5 to 100 micrometers. The presence of greater contact between modified clay and this polymer results in better clay dispersion inside the TPU matrix [37,38]. The clay fillers are homogeneously disseminated in the TPU matrix, and the surface film is coarsely rough, according to the photographs acquired. The high viscosity and cross-linking of the dispersed phase during solution polymerization can result in an uneven surface. The film surfaces of TPU and TPU with 1%, 3%, and 5% C25A nanocomposites have the best results in filler dispersion in TPU matrix, as evidenced by XRD spectra, according to the SEM pictures in Fig. 5. Exfoliation, intercalation, and aggregation are difficult to investigate decisively using SEM, which is easily reflected in XRD research. Fig. 5a has shown that 0 wt.% organoclay is smooth and compact, with no evidence of pores, whereas in Fig. 5b, the surface of TPU nanocomposites with 1 wt.% of organoclay is completely rough, which is attributed to the homogeneous distribution of the organoclay aggregate in the polymer matrix. The high viscosity and cross-linking of the dispersed phase during in situ polymerization can result in an uneven surface. Fig. 5c shows a micrograph of 3 wt.% of organoclay with the best dispersion of the organoclay. SEM images of TPU nanocomposite containing 5 wt.% Cl25A are shown in Fig. 5d, which shows a higher ratio of agglomerates.

Mechanical properties

The mechanical properties of TPU/C25A nanocomposites are summarized in Fig. 6. Tensile Strength (TS) and percent Elongation At Break (EB) test results are listed in Table 3. The tensile strength and elongation at break increases with an increase in the clay content up to 5 wt.% are shown in Fig. 6. In general, mixing Cloisite 25A and TPU has resulted in the diffusion of polymer chains into modified organophillic silicate layers and strong interfacial interactions. Hence it is expected that nanocomposites can tolerate more external load in comparison to the pure TPU. The tensile strength changed to 13.2 MPa which shown an 80% increment when 5% clay is added to TPU in comparison with pure TPU. This is due to the toughening and strengthening of TPU by the insertion of homogeneously dispersed clay in the TPU matrix. The TS and EB begin to decrease composites containing 7 wt.% due to the aggregation of clay content, causing a weak interaction between the TPU and clay layers.

Table 2: Mechanical data of TPU/C25A nanocomposites.

Sample Code	Tensile strength (MPa)	Young's Modulus (MPa)	Elongation at break (%)
TPU	7.8 ± 0.17	12.2 ± 0.82	658 ± 18
TPU/C25A-1	8.8 ± 0.22	18.3 ± 1.33	743 ± 32
TPU/C25A-3	11.6 ± 0.43	21.2 ± 2.76	810 ± 46
TPU/C25A-5	13.2 ± 0.68	24.3 ± 3.24	942 ± 51
TPU/C25A-7	12.8 ± 0.20	20.2 ± 2.68	902 ± 20

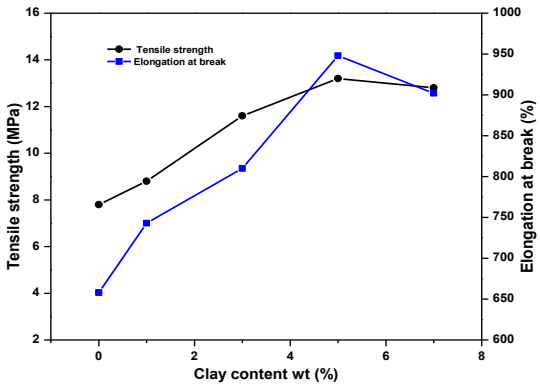

Fig. 6: Tensile strength and Elongation at break versus organoclay in TPU/C25A nanocomposites.

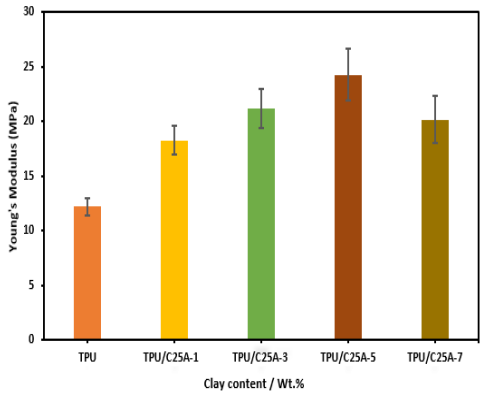

Fig. 7: Effect of clay concentration on Young's modulus in TPU/C25A nanocomposites.

Young's modulus of the nanocomposites with different clay wt.% and their error bar graph is shown in Fig. 7. Such results indicate that incorporating clay might reduce the molecular mobility of polymer chains, resulting in a less flexible material with a high Young's modulus. Results have proved that although nano clay showed a synergistic effect in tensile strength, they caused a significant reduction in polymer flexibilities [39,40].

Gas permeability adsorption study

The permeation study was done using the membrane separation unit at the constant pressure method. The oxygen permeability values of TPU/C25A nanocomposites are listed in Table 4. The TPU membrane is sealed within the two-pressure cell. High-pressure oxygen (1.5 bar) is kept in one cell and the other cell is maintained at atmospheric pressure. The amount of gas transported through the membrane is determined from the following tortuous path model or Nielsen model equation.

$$\frac{P}{P_0} = \frac{1-\varnothing_c}{1+\left(A_c/2\right)\varnothing_c} \quad (1)$$

Where P is the gas permeability of nanocomposite, P_0 is the gas permeability of polymer, $\emptyset_c$ is the volume fraction of the clay, and A_c is the average aspect ratio of clay respectively.

For TPU/C25A nanocomposite film, the oxygen and nitrogen permeability decreases with increasing clay loading, indicating that the organoclay enhances the oxygen and nitrogen barrier of the TPU. The diffusion coefficient of gases depends on the molecular size of the gas, rigidity, and mobility of polymer chains, and condensability of oxygen gas. Oxygen promotes higher solubility in the polymer due to the condensability of O_2 is 107K. The oxygen permeability is reduced by 56% with 5 wt.% of clay. When the clay loading is above 5 wt.% the barrier properties are reduced. Using the clay platelet dimensions we calculate the relative permeability for different clay stack numbers (N). The aspect ratio of the clay platelets is assumed to be 218 nm, the typical value for MMT. The permeation rate in oxygen and nitrogen gas with error bar graph was given in Fig. 8. The steady-state diffusion of solutes through many layered membranes loads with monodispersed fillers aligned in a regular array via the following equation [41-43].

Table 4: Oxygen and Nitrogen permeability coefficient of TPU/C25A nanocomposites.

Sample Code	Clay (Wt%)	Permeability coefficient (10^{-10}(STP)cmcm3 s^{-2} $cmHg^{-1}$)	
		Oxygen	Nitrogen
TPU	0	3.27 ± 0.42	3.26 ± 0.82
TPU/C25A	1	2.76 ± 0.62	3.02 ± 1.02
TPU/C25A	3	2.44 ± 0.98	2.68 ± 0.54
TPU/C25A	5	1.92 ± 0.76	2.12 ± 0.36
TPU/C25A	7	1.74 ± 0.57	1.83 ± 0.67

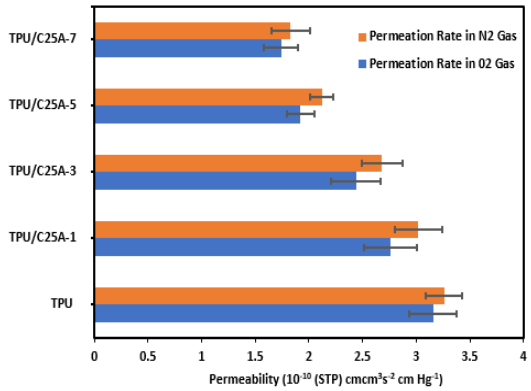

Fig. 8: Permeation rate in O_2, N_2 gas.

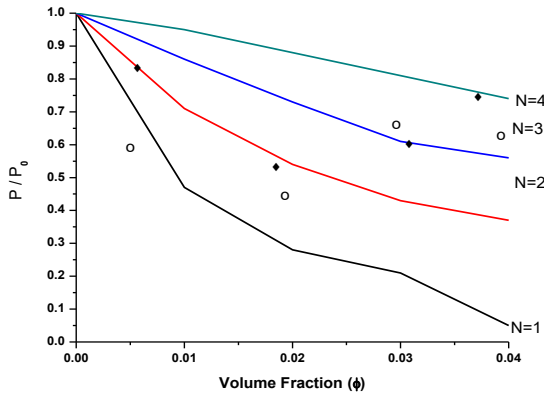

Fig. 9: The relative O_2, N_2 permeability of TPU/C25A nanocomposites as a function clay volume fraction for different clay stack numbers (N), — prediction of Eq. 1; ♦, • experimental data.

$$\frac{P}{P_0}=\frac{1-\varnothing}{1-\varnothing+\alpha\left(N^2\right)\varnothing^2} \qquad (2)$$

Nelson's tortuous model Eq. (1) predicts the stack number for TPU nanocomposites is around 2, as shown in Fig. 9. The major assumption made during the development of Eq. (2) is that the clay platelets are monodispersed and are aligned in a regular array.

CONCLUSIONS

TPU/C25A nanocomposites are prepared successfully by the solution polymerization method. The interaction between clay and polyurethane has proved the potential application of composite material to enhance oxygen and nitrogen permeability. FT-IR results have confirmed successful complexation and strong interaction between clay and polymer. The absence of a peak at $2\theta = 4.81^{o}$ in TPU/C25A in XRD analysis has indicated that the prepared nanocomposite is exfoliated and homogeneously dispersed in the polymer chain. SEM images show that the clay particles are equally dispersed inside the TPU matrix structure in the presence of tiny agglomerates, whereas the SEM images of pure TPU and TPU/C25A nanocomposites show significant variances. The results of TGA exhibited that the nanocomposite has higher thermal stability compared to TPU polymer. TGA results indicate that 85% of the initial clay added was quantitatively introduced into the TPU adduct as exfoliated structure and it might be changing the degradation mechanism of TPU/C25A nanocomposites under high temperature. Mechanical studies have also revealed that tensile strength and elongation at break increases with increasing clay content, while Young's modulus also increases. The TPU/C25A nanocomposite films have shown better barrier properties to oxygen than TPU due to the formation of the exfoliated nanostructure. The oxygen and nitrogen permeability coefficient of the TPU decreased after it was incorporated with clay. This enhancement in the barrier property is attributed to the clay content being well-dispersed in the polymer chain and improving the oxygen permeability by 56 %. It is concluded that the incorporation

of clay has successfully improved the barrier properties of TPU/C25A nanocomposites whereby this improvement may aid in packaging materials.

Acknowledgments

The authors would like to acknowledge the Research and Development Centre Bharathiar University for support and the Central Leather Research Institute (CLRI) for all the analysis.

Received : Aug. 7, 2021 ; Accepted : Dec. 27, 2021

REFERENCES

[1] Dorigato A., Pegoretti A., Penati A., Effect of the Polymer—Filler Interaction on the Thermo-Mechanical Response of Polyurethane-Clay Nanocomposites from Blocked Prepolymer, *J. Rein. Plast. Compos.*, **30**: 325-335 (2011).

[2] Allami, T., Alamiery, A., Nassir, M.H., Kadhum, A.H., Investigating Physio-Thermo-Mechanical Properties of Polyurethane and Thermoplastics Nanocomposite in Various Applications, *Polym.* **13**: 2467-2491 (2021).

[3] Khalifa M., Anandhan S., Wuzella G., Lammer H., Mahendran A., Thermoplastic Polyurethane Composites Reinforced with Renewable and Sustainable Fillers–A Review, *Polym. Technol. Mater.*, **59**: 1751-1769 (2020).

[4] Ali F., Ullah H., Ali Z., Rahim F., Khan F., Ur Rehman Z., Polymer-Clay Nanocomposites, Preparations and Current Applications: A Review, *Current Nanomaterials.*, **1**: 83–95 (2016).

[5] Chaitoglou S., Spachis L., Zisis G., Raptis I., Papanikolaou N., Vavouliotis A., Penedo R., Fernandes N., Dimoulas A., Layer-by-Layer Assembled Graphene Coatings on Polyurethane Films as He Permeation Barrier, *Prog. Org. Coat.*, **150**: 105984-105991 (2021).

[6] Merillas B., Villafañe F., Rodríguez-Pérez M.Á., Nanoparticles Addition in PU Foams: The Dramatic Effect of Trapped-Air on Nucleation, *Polym.* **13**: 2952-2963 (2021).

[7] Gul S., Kausar A., Muhammad B., Jabeen S., Research Progress on Properties and Applications of Polymer/Clay Nanocomposite, *Polym. Plast. Technol. Eng.*, **55**: 684-703 (2016).

[8] Samyn F., Bourbigot S., Jama C., Bellayer S., Fire Retardancy of Polymer Clay Nanocomposites: Is there an Influence of the Nanomorphology?, *J. Polym. Degrad. Stab.*, **93**: 2019-2024 (2008).

[9] Saliney T., Shaji T., Jiji A., Soney C.G., Sabu T., Investigation of the Mechanical, Thermal and Transport Properties of NR/NBR Blends: Impact of Organoclay Content, *J. Polym. Res.*, **25**: 165-175 (2018).

[10] Kiliaris P., Papaspyrides C.D., Polymer/Layered Silicate (Clay) Nanocomposites: An overview of Flame Retardancy, *Prog. Polym. Sci.*, **35**: 902-958 (2010).

[11] Skleničková K., Vlčková V., Abbrent S., Bujok S., Paruzel A., Kanizsová L., Trhlíková O., Říhová Ambrožová J., Halecký M., Beneš H., Open-Cell Aliphatic Polyurethane Foams with High Content of Polysaccharides: Structure, Degradation, and Ecotoxicity, *ACS Sustainable Chem.Eng.*, **9**: 6023-6032 (2021).

[12] Maji P.K., Das N.K., Bhowmick A.K., Preparation and Properties of Polyurethane Nanocomposites of Novel Architecture as Advanced Barrier Materials, *Polym.*, **51**: 1100-1110 (2010).

[13] Barick A.K., Tripathy D.K., Effect of Organically Modified Layered Silicate Nanoclay on the Dynamic Viscoelastic Properties of Thermoplastic Polyurethane Nanocomposites, *Appl. Clay. Sci.*, **52**: 312-321 (2011).

[14] Alhanish A., Abu Ghalia M., Biobased Thermoplastic Polyurethanes and Their Capability to Biodegradation, *Eco-Friendly Adhesives for Wood and Natural Fiber Composites*, Springer, 85-104 (2021).

[15] Adak B., Joshi M., Butola B.S., Polyurethane/Clay Nanocomposites with Improved Helium Gas Barrier and Mechanical Properties: Direct Versus Master-Batch Melt Mixing Route, *J. Appl. Polym. Sci.*, **135**: 46422- (2018).

[16] Salahuddin N., Abo-El-Enin S.A., Selim A., Salah El-Dien O., Synthesis and Characterization of Polyurethane/Organo-Montmorillonite Nanocomposite, *Appl. Clay. Sci.*, **47**: 242-48 (2010).

[17] Reddy G.V.R., Joshi M., Adak B., Deopura B.L., Studies on the Dyeability and Dyeing Mechanism of Polyurethane/Clay Nanocomposite Filaments with Acid, Basic and Reactive Dyes, *Coloration. Technol.*, **134**: 117-125 (2018).

[18] Stefanovic I.S., Spirkova M., Ostojic S., Stefanov P., Pavlovic V., Pergal M.V., Montmorillonite /Poly(Urethane-Siloxane) Nanocomposites: Morphological, Thermal, Mechanical and Surface Properties, *Appl. Clay. Sci.*, **149**: 136-146 (2017).

[19] Uhl F.M., Davuluri S., Wong S., Webster D., Organically Modified Montmorillonites in UV Curable Urethane Acrylate Films, *Polym.*, **45**: 175-187 (2004).

[20] Sariyeh P., Mohammad S., Farshad K., Mehrdad K., Polyethylene/Clay/Graphite Nanocomposites as Potential Materials for Preparation of Reinforced Conductive Natural Gas Transfer Pipes, *Iran. J. Chem. Chem. Eng. (IJCCE)*, **39**: 59-68 (2020).

[21] Marcano A., Fatyeyeva K., Koun M., Dubuis P., Grimme M., Marais S., Recent Development in the Field of Barrier and Permeability Properties of Segmented Polyurethane Elastomers, *Rev. Chem. Eng.*, **35**: 445-474 (2019).

[22] Herrera -Alonso J.M., Marand E., Little J.C., Cox S.S., Transport Properties in Polyurethane/Clay Nanocomposites as Barrier Materials: Effect of Processing Conditions, *J. Membrane. Sci.*, **337**: 208-214 (2009).

[23] Alobad Z.K., Albozahid M., Naji H.Z., Alrheem H.S., Saiani A., Influence of Hard Segments Content on Thermal, Morphological and Mechanical Properties of Homo and Co-Polyurethanes: A Comparative Study, *Arch. Mater. Sci. Eng.*, **1**: 5-16 (2021).

[24] Kim H., Mitura Y., Mascosko C.W., Graphene/Polyurethane Nanocomposites for Improved Gas Barrier and Electrical Conductivity, *Chem. Mater.*, **22**: 3441-3450 (2010).

[25] Peretz Damari S., Cullari L., Nadiv R., Nir Y., Laredo D., Grunlan J., Regev O., Graphene Induced Enhancement of Water Vapor Barrier in Polymer Nanocomposites, *Compos. B: Eng.*, **134**: 218-224 (2018).

[26] Reza J., Behnam E., Hamed T., Effects of Cellular Morphology and Water Absorption Capacity of Poly(vinyl alcohol) Foam, *Iran. J.Chem.Chem. Eng. (IJCCE)*, **36**: 59-67 (2017).

[27] Amari A., Alzahrani F.M.A., Katubi K.M., Alsaiari N.S., Tahoon M.A., Rebah F.B., Herrera-Alonso., Marand E., Little J.C., Clay-Polymer Nanocomposites: Preparations and Utilization for Pollutants Removal, *Materials.*, **14**: 1365-1386 (2021).

[28] Gholami M., Sadeghi G.M., Investigating the Effects of Chemical Modification of Clay Nanoparticles on Thermal Degradation and Mechanical Properties of TPU/Nanoclay Composites, *J. Particle. Science Technol.*, **1**: 7-15 (2015).

[29] Adak B., Butola B.S., Joshi M., Effect of Organoclay-Type and Clay-Polyurethane Interaction Chemistry for Tuning the Morphology, Gas Barrier and Mechanical Properties of Clay/Polyurethane Nanocomposites, *Appl. Clay. Sci.*, **161**: 343-353 (2018).

[30] Behjat T., Najmeh R., Preparation and Characterization (Mechanical and Water Absorpion Properties) of CMC/PVA/Clay Nanocomposite Films, *Iran. J. Chem. Chem. Eng. (IJCCE)*, **35**: 9-15 (2016).

[31] Ramesh S., Punithamurthy K., The Effect of Organoclay on Thermal and Mechanical Behaviours of Thermoplastic Polyurethane Nanocomposites, *Dig. J. Nanomater. Biostruct.*, **12**: 331-338 (2017).

[32] Zeng Q.H., Wang D.Z., Yu A.B., Lu G.Q., Synthesis of Polymer-Montmorillonite Nanocomposites by in situ Intercalative Polymerization, *Nanotech.*, **13**: 549-553 (2002).

[33] Rathi S., Dahiya J.B., Polyammide 66/Nanoclay Composites: Synthesis, Thermal and Flammability Properties, *Adv. Mat. Lett.*, **3**: 381-387 (2012).

[34] Rafiee M., Nitzsche F., Laliberte J., Hind S., Robitaille F., Labrosse MR., Thermal Properties of Doubly Reinforced Fiberglass/Epoxy Composites with Graphene Nanoplatelets, Graphene Oxide and Reduced-Graphene Oxide, *Compos. B: Eng.*, **164**: 1–9 (2019).

[35] Poornima Vijayan P., Debora P., Pournami V.P., Jose M., Thomas K.S., The Role of Clay Modifier on Cure Characteristics and Properties of Epoxy/Clay/ Carboxyl-Terminated Poly(butadiene-co-acrylonitrile) (CTBN) Hybrid, *Materials Technology: Advance Performance Materials.*, **32**: 171-77 (2017).

[36] Chandran N., Chandran S., Hanna J.M., Thomas S., Compatiblizing Action and Localization of Clay in a Polypropylene/Natural Rubber (PP/NR) Blend, *RSC Adv.*, **5**: 86265-86273 (2015).

[37] Joshi M, Adak B., Butola B.S., Polyurethane Nanocomposite Based Gas Barrier Films, Membranes and Coatings: A Review on Synthesis, Characterization and Potential Applications, *Prog. Mater. Sci.*, **97**: 230-282 (2018).

[38] Poornima Vijayan P., Debora P., Jose M.K., Thomas S., Effect of Organically Modified Nanoclay on the Miscibility, Rheology, Morphology and Properties of Epoxy/Carboxyl-Terminated (Butadiene-co-Acrylonitrile) Blend, *Soft Matter.*, **9**: 2899-2911 (2013).

[39] Mustapha K., Mederic P., Lynda Z., Grohens Y., Bruzaud S., Influence of Loading Rates on Morphology and Mechanical Properties of PLA/Clay Nanocomposites, *Int. J. Microstructure and Materials Properties.*, **7**: 390-399 (2012).

[40] Ahmadi Y., Yadav M., Ahmad S., Oleo-Polyurethane-Carbon Nanocomposites: Effects of in-situ Polymerization and Sustainable Precursor on Structure, Mechanical, Thermal, and Antimicrobial Surface-Activity, *Compos. B: Eng.*, **164**: 683-692 (2019).

[41] Kalendova A., Merinska D., Gerard J. F., Slouf M., Polymer/Clay Nanocomposites and their Gas Barrier Properties, *Polym. Compos*., **34**: 1418–1424 (2013).

[42] Goodarzi V., Jafari S.H., Khonakdar H.A., Ghalei B., Assessment of Role of Morphology in Gas Permselectivity of Membranes Based on Polypropylene/Ethylene Vinyl Acetate/Clay Nanocomposite, *J. Memb. Sci.*, **445**: 76-87 (2013).

[43] Wan J., Bi W., Liao X., Xiao H., Chen X., Chen J., Gas Diffusion in Polymer Nanocomposites: Role of Defects and Caves in Fillers, *J. Polym. Res.*, **28**: 368 (2021).